

# Shot Noise at Hopping: A Numerical Study

Yusuf A. Kinkhabwala, Viktor A. Sverdlov, and Konstantin K. Likharev  
 Department of Physics and Astronomy,  
 Stony Brook University, Stony Brook, NY 11794-3800

Alexander N. Krotkov  
 Department of Electrical Engineering,  
 University of California - Riverside, Riverside, CA 92521

(Dated: May 16, 2019)

We have carried out extensive Monte-Carlo simulations of 2D hopping (without Coulomb interaction account) in a system with a completely random distribution of localized sites in both space and energy, for a broad range of the applied electric field  $E$  and temperature  $T$ , both within and beyond the variable-range-hopping region. The calculated properties include dc current, statistics of localized site occupation and hop lengths, and shot noise intensity. For sufficiently large samples, the Fano factor scales with length  $L$  as  $(L_c/L)^\alpha$ , where  $\alpha = 0.76 \pm 0.08$ . The electric field dependence of parameter  $L_c$  (interpreted as the critical cluster length) is compatible with the law  $L_c / E^{0.911}$  following from percolation theory arguments at relatively low  $E$ , but attens and approaches the average hop length in very high fields.

PACS numbers: 72.20.Ee, 72.20.Ht, 73.50.Td

## I. INTRODUCTION

Theory of hopping transport in disordered conductors,<sup>1,2,3</sup> without account of electron-electron interaction, is considered as a well established (if not completed) field, the recent research being focused mostly on Coulomb effects. Two factors, however, have motivated us to have a new look at this subject:

1. Relatively recently it was recognized that shot noise<sup>4</sup> is a very important characteristic of electron transport. In particular, the suppression of current fluctuation density  $S_I(1)$  at low frequencies, relative to its Schottky formula value  $2e^2h^2I$ , is a necessary condition for the so-called sub-electron (quasi-continuous) charge transfer.<sup>5</sup> Preliminary calculations of shot noise at 1D<sup>6</sup> and 2D<sup>7</sup> hopping have shown that such suppression may, indeed, take place. However, the calculations of this effect for the most important 2D case have been limited to just one particular value of electric field, at zero temperature.<sup>7</sup> It was important to examine whether the law governing this suppression is really as general as it seemed.

2. The literature is surprisingly scarce of quantitative data on major characteristics of hopping, especially in the high-electric-field region ( $eE \gg k_B T$ ) where dc conductivity becomes a substantial function of  $E$ . General arguments of the variable-range-hopping theory<sup>8</sup> indicate that in this region the field dependence for 2D hopping should be close to

$$= A_{E_0} \exp \left( -B_{E_0} \frac{E_0}{E} \right)^{\frac{1}{1-\beta}}; \quad (1)$$

where  $E_0$  and  $E_0$  are the natural units of and  $E$ . Also, to the best of our knowledge, the exact range of valid-

ity of Eq. (1) and the location of the crossover to field-independent conductivity (at finite temperature) have never been established. This is not very surprising because virtually the only theoretical technique available for hopping characterization in the high-field region is Monte Carlo modeling, which requires high-performance computing. For example, the work reported below took about a million node-hours on modern supercomputers. Such computing resources have become available for the academic solid state physics community only recently.

## II. MODEL

We have studied 2D rectangular ( $L \times W$ ) samples with "open" boundary conditions on the interface with well-conducting electrodes<sup>7</sup> - see inset in Fig. 1. In the present study, we have concentrated on the broad samples with width  $W = L_c$ , where  $L_c$  is the effective percolation cluster size (see below). The localized sites are randomly distributed over the sample area, while the localized state energies  $\epsilon_j$  are randomly distributed over a sufficiently broad energy band, so that the 2D density of states is constant at all energies relevant for conduction. Electrons can hop from any site  $j$  to any other site  $k$  with the rate

$$r_{jk} = r_{jk} \exp \left( -\frac{r_{jk}}{a} \right); \quad (2)$$

Such exponential dependence on the hop length has been assumed in virtually all theoretical studies of hopping.<sup>9</sup> However, in contrast to most other authors, we take Eq. (2) literally even at small distances  $r_{jk} \ll a$ ; this is

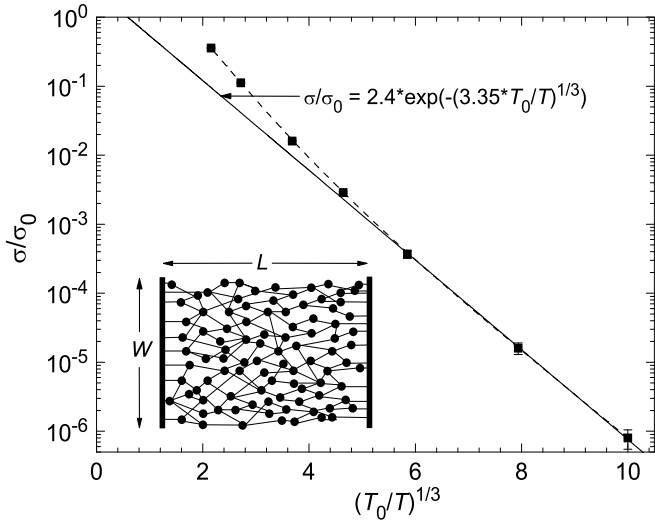


FIG. 1: Linear conductivity as a function of temperature  $T$ . Points show the results of averaging over 80 samples varying in size ( $L \times W$ ) from  $20 \times 10 \text{ \AA}$  to  $160 \times 100 \text{ \AA}^2$ , biased by a low electric field  $E = E_T$ . Dashed lines are just guides for the eye, while the straight line corresponds to the best fit of the data by Eq. (7). Constants  $T_0$  and  $\sigma_0$  are defined by Eqs. (5) and Eq. (6), respectively. The inset shows the system under analysis (schematically).

important only at very high fields and/or temperatures where the average value of  $r_{jk}$  becomes comparable to  $a$ . Of course our qualitative results for this region, are only true for the specific conning potential.

A nother distinction from most other works in this field is that we assume that the hopping rate amplitude  $r_{jk}$  depends continuously on the localized site energy difference  $E_{jk} = E_j - E_k + eE$ :

$$r_{jk}(E_{jk}) = g \frac{e^{-\frac{|E_{jk}|}{k_B T}}}{1 + \exp \left( \frac{|E_{jk}|}{k_B T} \right)}; \quad (3)$$

We believe that this model is much more natural than the usual "Metropolis" dependence having a cusp at  $E_{jk} = 0$ , while Eq. (3) still satisfies the Gibbs detailed balance requirement  $r_{jk} = r_{kj} \exp(-|E_{jk}|/k_B T)$ .

The interaction of hopping electrons is assumed negligible, with the exception of the implicit Pauli principle interaction, i.e. no hopping to already occupied sites.

Scales of all variables within our model are natural combinations of the constants  $a$  and  $(\text{plus temperature } T, \text{ applied electric field } E, \text{ and fundamental constants})$ . In particular, there are three possible energy scales:  $k_B T$ ,  $eEa$ , and  $a^2$ . This means that there are two characteristic values of electric field:

$$E_T = \frac{k_B T}{ea}; E_0 = \frac{1}{e a^2}; \quad (4)$$

We will be mostly interested in the case of low temperatures,  $T < T_0$ , where

$$T_0 = \frac{1}{k_B a^2} \quad (5)$$

is the field-independent scale of temperature, so that  $E_T < E_0$ .

Note that the only role of the dimensionless parameter introduced by Eq. (3) is to participate in the scale of hopping conductivity

$$\sigma_0 = \frac{e^2}{g a^2}; \quad (6)$$

In order to keep coherent quantum effects leading to weak localization and metal-to-insulator transition negligibly small, and hence the formulated hopping model possible,  $g$  should be much less than unity.

The dynamic Monte Carlo calculations were carried out using the algorithm suggested by Bakhvalov et al.,<sup>10</sup> which has become the de-facto standard for single-electron tunneling simulations.<sup>11</sup> All calculated variables were averaged over the sample, and in most cases, over several (many) samples with independent random distributions of localized sites in space and energy, but with the same dimensionless parameters  $L=a$ ,  $W=a$ ,  $T=T_0$ , and  $E=E_0$ . For the purposes of this work, the noise spectral density calculation technique has been modified.<sup>12</sup>

### III. DC CURRENT AND HOPPING STATISTICS

In order to understand the relation between our model and the prior results in this field, we have started from the calculation of dc current  $I$  as a function of  $T$  and  $E$ . If the electric field is small,  $E = E_T$ , then the current is proportional to  $E$ , and the transport is completely characterized by the linear conductivity  $\sigma = I/E$ . Fig. 1 shows the calculated conductivity as a function of temperature  $T$ ; in the whole region  $T < T_0$  this dependence follows the 2D Mott law<sup>1,2,3</sup>

$$I = A_{T_0} \exp \left( -B_T \frac{T_0}{T} \right)^{\frac{1}{1+3}}; \quad (7)$$

within the accuracy of our numerical experiments. For the constants participating in this expression, fitting gives the following values

$$A_{T_0} = 2.4 \quad 0.1; B_T = 3.35 \quad 0.12; \quad (8)$$

This result for  $B_T$  should be compared with the following values reported in the literature: 2.2<sup>13</sup>, 3.45<sup>2</sup>, and 3.25.<sup>14</sup> The differences are probably due to those of the used models (see Sec. II above).

At higher electric fields ( $E > E_T$ ), dc current starts to grow faster than the Ohm law, so that if we still keep the above definition of conductivity, it starts to grow with  $E$  (Fig. 2). At  $T = 0$ , the results are well described by Eq. (1) with

$$A_E = 0.050 \quad 0.005; B_E = 0.906 \quad 0.015; \quad (9)$$

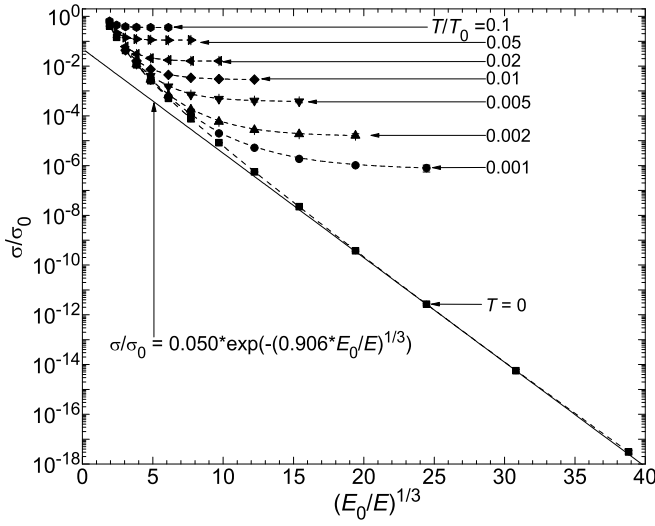


FIG. 2: Nonlinear conductivity  $\sigma/\sigma_0$  as a function of electric field  $E$  for several values of temperature  $T$ . Each point represents data averaged over 80 samples of the same size (ranging from  $20-14 \text{ \AA}^2$  to  $1000-700 \text{ \AA}^2$ , depending on  $T$  and  $E$ ). Dashed lines are only guides for the eye; while the straight line shows Eq. (1) with the best-fit values of  $A_E$  and  $B_E$ .

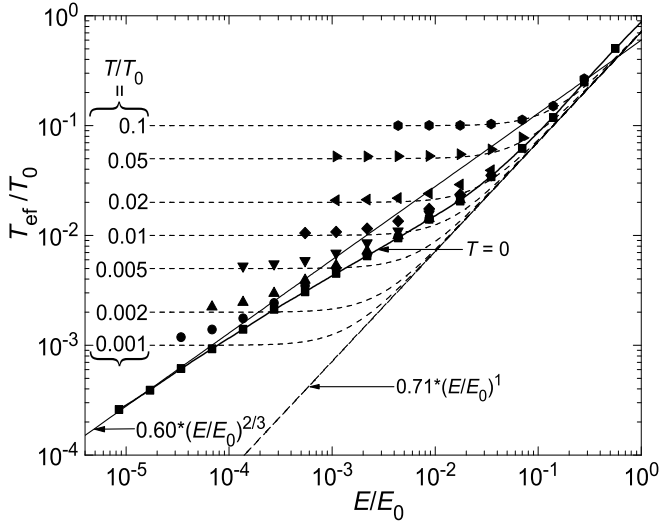


FIG. 3: The effective temperature of current carriers as a function of electric field for several values of temperature. Closed points: Monte Carlo (MC) simulation results; dashed lines: master equation (ME) results. The solid curve along  $T = 0$  is only a guide for the eye.

These values are an improvement on Ref. 7 where  $A_E = 1.1$  and  $B_E = 1.27$  are determined from a narrower range of electric fields.

Finally, Fig. 2 shows that when the electric field becomes comparable with the value  $E_0$  defined by the second of Eqs. (4), dc current and hence, conductivity start to grow even faster than given by Eq. (1).

In order to understand the physics of hopping in these three field regions better, it is very useful to have a look at the statistics of localized site occupation and hopping length. We have found that for all studied values of  $E$  and  $T$ , the probability of site occupation closely follows the Fermi distribution with the local Fermi level

$$\langle r \rangle = L \exp(-E_F r) \quad (10)$$

(where  $L$  is the Fermi level of the source electrode) and some effective temperature  $T_{\text{eff}}$ . Points in Fig. 3 show  $T_{\text{eff}}$  as a function of electric field  $E$  for several values of physical temperature  $T$ . Dashed, dotted, and dash-dotted lines show the result of the best fitting of the naive single-particle master equation

$$\frac{\partial f(\mathbf{r}; t)}{\partial t} = \frac{Z}{d^2 r} \frac{Z}{d^0} \exp \left( \frac{-r}{a} \right) \left[ f^0 + eE_F r f^0 \right] - \left[ f^0 + \left( \frac{Z}{d^0} - eE_F r \right) f^0 \right] \left[ 1 - f(\mathbf{r}; t) \right] g \quad (11)$$

by a stationary Fermi distribution. Eq. (11) would follow from our model if percolation effects were not substantial. At real hopping, we can expect the results following from Eq. (11) to be valid only in certain limits.<sup>15</sup> For example, in the low field limit,  $E \rightarrow 0$ , both methods give  $T_{\text{eff}} = T$ . At higher fields the effective temperature grows with the field which "overheats" electrons. At very high fields ( $E = E_0 > 0.3$ ) both methods agree again and give

$$k_B T_{\text{eff}} = C e E_F a; \quad C = 0.71 \quad 0.02; \quad (12)$$

A similar result, but with  $C = 1.34$ , for our definition of  $a$ , was obtained by Marianer and Shklovskii<sup>16</sup> for a rather different model with an exponential energy dependence of the density of states. However, at the intermediate fields  $E_T \ll E \ll E_0$  (this regime is frequently called the "high-field variable-range-hopping"), the master equation still gives the same result Eq. (12) and hence fails to appreciate that in fact  $T_{\text{eff}}$  is proportional to  $E^{2/3}$ . In order to explain this result, let us discuss the statistics of hop lengths (Figs. 4 and 5).

The two- and one-dimensional histograms in Fig. 4 show the probability density  $P$  of a hop between two sites separated by the vector  $\mathbf{r}$ , and also the density  $P_d$  weighed by the factor  $\frac{1}{N_{jk}} \frac{N_{kj}}{N_{kj}}$  where each  $N$  is the total number of hops (during a certain time interval) in the indicated direction. The latter weighting emphasizes the site pairs  $(j; k)$  contributing substantially to the net hopping transport, in comparison with "blinking" pairs just exchanging electrons without their advance along the field. It is clear that at relatively high temperatures or low fields ( $E \ll E_T$ ) the non-weighted distribution should be symmetric (Fig. 4a). Fig. 4d shows that in this case the one-dimensional probability density is well approximated by the Rayleigh distribution,  $P(r) / r \exp(-r/a)$ . However, the weighed hop distribution is strongly asymmetric even in the limit  $E \rightarrow 0$  (Fig. 4b). This asymmetry is even more evident at low

temperatures or high fields ( $E = E_T$ ); in this case the distribution has a sharp boundary (Fig. 4c). Fig. 4d shows those cases where the 1D histograms deviate substantially from the distribution predicted by the master equation (see Eq. (19)).

Figure 5 shows the rms non-weighted ( $r_{rm,s}$ ) and direction-weighted ( $r_{rm,ds}$ ) hop lengths, defined, respectively, as

$$r_{rm,s} = \frac{\int_{jk}^P r_{jk}^2 N_{jk} + r_{kj}^2 N_{kj}}{\int_{jk}^P (N_{jk} + N_{kj})} \quad (13)$$

and

$$r_{rm,ds} = \frac{\int_{jk}^P r_{jk}^2 N_{jk} r_{kj}^2 N_{kj}}{\int_{jk}^P N_{jk} N_{kj}} \quad (14)$$

(that are of course just the averages of the histograms shown in Fig. 4), as functions of applied electric field for several values of temperature. At  $T = 0$ , hopping is strictly one-directional (i.e., if  $N_{jk} \neq 0$ , then  $N_{kj} = 0$ ), so that  $r_{rm,s}$  and  $r_{rm,ds}$  should be equal. In fact, simulation shows that in this limit both lengths coincide, at lower fields following the scaling<sup>8</sup>

$$r_{rm,s} = r_{rm,ds} = D a \frac{E_0^{1=3}}{E} \quad ; \quad E_T = E = E_0; \quad (15)$$

with  $D = 0.72 \pm 0.01$ . We are not aware of any values with which  $D$  should be compared.

This scaling of  $r$  in the variable-range-hopping region is essentially the reason for the scaling of  $T_{ef}$  mentioned above; in fact, the hopping electron gas overheating may be estimated by equating  $k_B T_{ef}$  to the energy gain  $eE r_{rm,s}$ , possibly multiplied by a constant of the order of one. For the effective temperature, this estimate gives

$$k_B T_{ef} = \text{const } eE r_{rm,s} = G e a E_0^{1=3} E^{2=3} = G \frac{(E = E_0)^{2=3}}{a^2}; \quad (16)$$

in accordance with the result shown in Fig. 3. For the constant  $G$  our Monte Carlo simulations give the value  $0.60 \pm 0.02$ ; we are not aware of any previous results this number could be compared with.

At higher fields ( $E > 0.1E_0$ ) the hop lengths start to decrease slower, approaching a few localization lengths  $a$  (Fig. 5a). In this ("ultra-high-field") regime, the energy range  $eEa$  for tunneling at distances of a few  $a$  is so high that there are always some accessible empty sites within this range, so that long hops, dominant at variable range hopping, do not contribute much into conduction.

At finite temperatures, the most curious result is a non-monotonic dependence of the rms hopping length on the applied field — see Fig. 5a. At  $E = 0$ ,  $r_{rm,s}$  has to be field-independent, and there is no scale for it besides  $a$ . (As evident as it may seem, this fact is sometimes missed in popular descriptions of hopping.) In order to make

a crude estimate of  $r_{rm,s}$  in this limit, one can use the master equation Eq. (11). In this approach, at thermal equilibrium (i.e. at  $T$  independent of  $r$ ), the hop length probability density  $P(r)$  can be found as

$$P(r) = 2r d \int_0^r \exp \frac{-r}{a} [f(0)f(1) - f(0)f(1)] + \int_0^r [f(0)f(1) - f(0)f(1)] g / r \exp \frac{-r}{a}; \quad (17)$$

in a good agreement with the results shown in Fig. 4d for this case. From Eq. (17), we get

$$r_{rm,s} = r^2 \stackrel{1=2}{=} \frac{\int_0^R P(r) r^2 dr}{\int_0^R P(r) dr} \stackrel{1=2}{=} \frac{P}{6a} = 2.45a; \quad (18)$$

in a good agreement with numerical data shown in Fig. 5.

A similar calculation for  $r_{rm,ds}$  may be obtained by expanding the tunneling rate  $(e^0 + eE r)$  in small electric field as  $(e^0 + eE r)^0 (e^0 + eE r)^1$ . The result is

$$P_d(r) = eE r^2 \int_0^r \int_0^s \int_0^j d \int_0^s d \int_0^j d \int_0^s d \int_0^r \exp \frac{-r}{a} [f(0)f(1) - f(0)f(1)] + [f(0)f(1) - f(0)f(1)] g; \\ P_d(r) / r^2 \exp \frac{-r}{a}; \\ r_{rm,ds} = \frac{\int_0^R P_d(r) r^2 dr}{\int_0^R P_d(r) dr} \stackrel{1=2}{=} \frac{P}{12a} = 3.46a; \quad (19)$$

The Monte Carlo data (Fig. 5), however, differ from this result, showing that at  $E = 0$ ,  $r_{rm,ds}$  obeys the Mott law<sup>1,2,3</sup>

$$r_{rm,ds} = H a \frac{T_0^{1=3}}{T} + I a; \quad T = T_0; \quad (20)$$

with the best-fit values  $H = 0.52 \pm 0.05$  and  $I = 2.0 \pm 0.1$ <sup>17</sup>. In contrast, the function  $r_{rm,s}(T)$  is rather far from Eq. (20), because the Mott law refers to long hops responsible for transport (with the average approximately corresponding to  $r_{rm,ds}$ ), while  $r_{rm,s}$  reflects the statistics of all hops.

To summarize, our results for average conductivity and hop statistics confirm that our model gives a reasonable description of the well-known picture of hopping, including the usual variable range hopping at low fields ( $E = E_T$ ) and "high-field variable range hopping" at  $E = E_0$ . Moreover, the model also describes the "ultra-high-field" region ( $E = E_0$ ) where the variable range hopping picture is no longer valid, since from most localized sites an electron can hop, with comparable probability, to several close sites. In the last regime, there is no single percolation cluster in any local region of the sample; rather, electrons follow a large number of intervening trajectories.

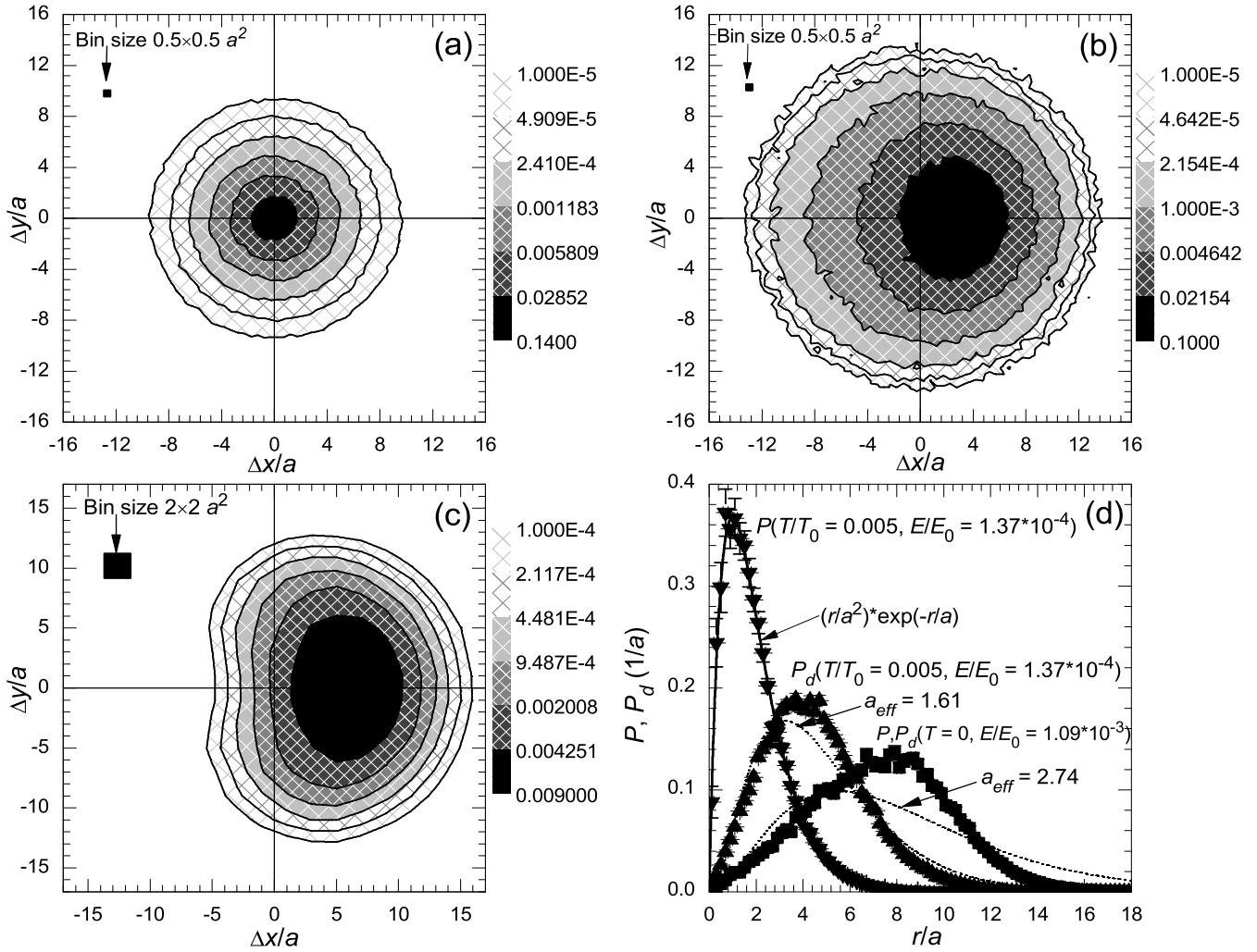


FIG. 4: (a)–(c) Two-dimensional and (d) one-dimensional histograms of hop lengths for two typical cases: (a) and (b):  $T=T_0=5 \times 10^{-3}$ ,  $E=E_0=1.37 \times 10^{-4}$  ( $E=E_T$ ) and (c):  $T=0$ ,  $E=E_0=1.09 \times 10^{-3}$  ( $E_T=E$ ). The vertical (shade-coded) scale in panels (a) and (c) is proportional to the probability  $P$  of hops with given  $r=(x; y)$ , while that in panel (b), to the probability  $P_d$  weighed by factor  $\sqrt{N_{jk}}/N_{kj,j}$ —see the text. (Since at  $T=0$  there are no backward hops, for the case shown in panel (c),  $P$  and  $P_d$  coincide.) Panel (d) shows  $P$  and  $P_d$ , averaged over all angles of vector  $r$ , for both the high-eld and low-eld case. Dashed lines show the distribution (19) given by master equation, for best-fit values of  $a_{\text{eff}}$ .

#### IV. SHOT NOISE

The achieved understanding of hopping (within our model) has helped us to interpret the results of shot noise simulation. This simulation was, naturally, limited to the case of low temperatures,  $E_T \ll E$ . (In the opposite limit, noise is described by the fluctuation-dissipation theorem, its low-frequency intensity can be found from (17) and does not require a special calculation.)

Figure 6 shows a typical dependence of the current noise spectral density  $S_I$  on the observation frequency  $\omega$ . In contrast with the case of substantial electron-electron interaction, which may lead to highly colored ( $1/f$ -type) noise,<sup>18,19,20,21</sup> hopping of non-interacting electrons results in white noise at relatively low frequen-

cies and hence, to a well-defined Fano factor

$$F = \frac{S_I(0)}{2e\hbar I}; \quad (21)$$

which is the commonly accepted characterization of shot noise.<sup>4</sup> The largest practical problem with the calculation of the Fano factor is that its meaningful averaging typically requires either larger sample size, or larger statistical ensemble of random samples, or both. This problem is illustrated in Fig. 7 which shows typical histograms of  $F$  and dc conductivity for samples of various size  $L \times W$ . One can see that for sufficiently large and wide samples the Fano factor distribution is typically wider than that of  $I$ , and for small samples the notion of statistical average  $F$  may be rather superficial. In order to

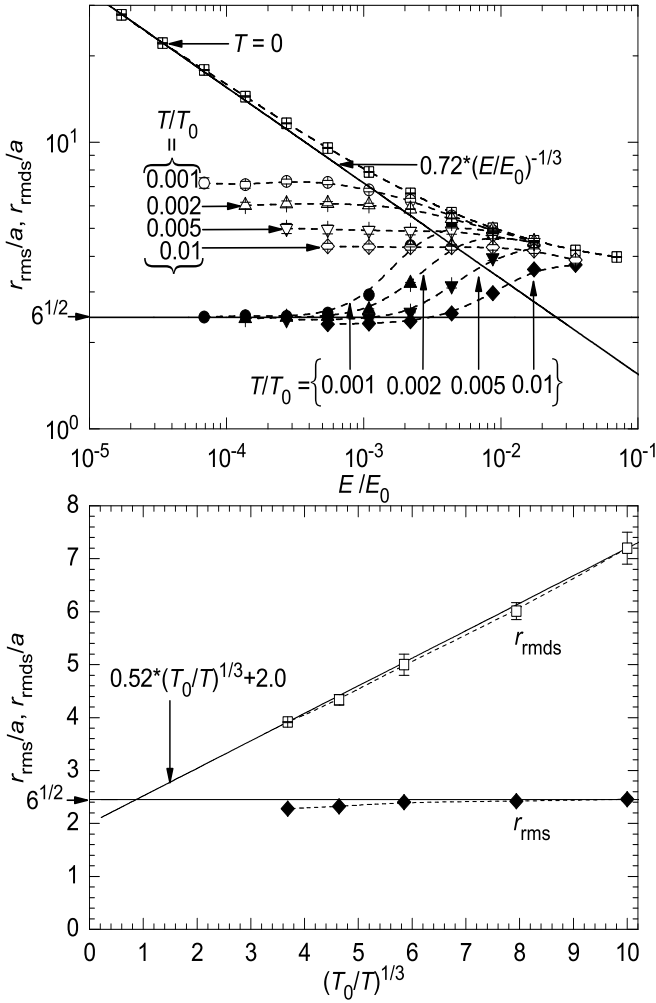


FIG. 5: R m s. hop length  $r_{\text{rms}}$  (solid points) and the weighed average length  $r_{\text{rmds}}$  (open points) as functions of (a) applied electric field  $E$  for several temperatures  $T$ , and (b) of tem perature at  $E = 0$ . T tilted straight lines in panels (a) and (b) show the best ts by Eqs. (15) and (20), respectively, while the horizontal thin lines show the values following from the m aster equation. Curves are only guides for the eye.

circum vent this problem at least partly, in this study we have focused on the Fano factor dependence on sample length  $L$ , always taking the sam ples much wider than the critical cluster size  $L_c$ . (For the de nition of the cluster length  $L_c$ , see the text and Fig. 9 below). Even with this restriction, and an advanced algorithm for spectral density calculation,<sup>12</sup> getting hF i with sensible error bars has required very substantial supercomputer resources.

Figure 8 shows our main result, the average Fano factor as a function of  $L$  for several values of the applied electric field. This gure shows that the results may be reasonably well twi with a universal dependence on  $L=L_c$ , that approaches<sup>7</sup>

$$hF i = \frac{L_c}{L} ; \quad L \gg L_c : \quad (22)$$

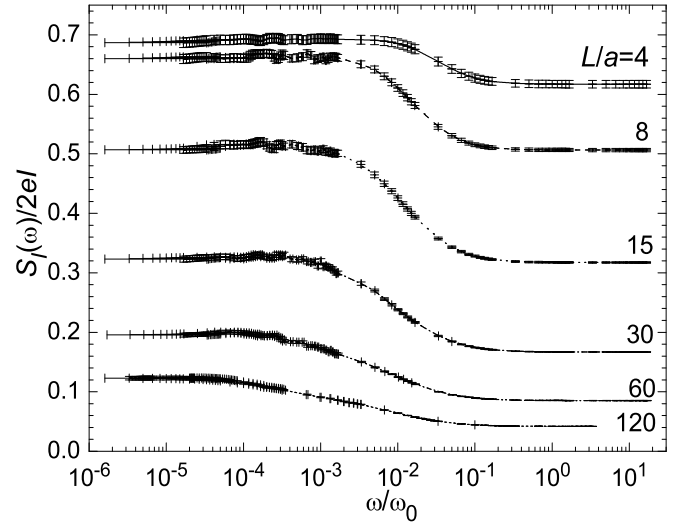


FIG. 6: Spectral density  $S_i$  of current uctuations as a function of observation frequency  $\omega$ , measured in units of  $\omega_0 = (I=e) = (W=a)$ , for several values of sample length  $L$ . Parameters:  $E = E_0 = 8.75 \cdot 10^3$ ,  $W = a = 60$ ,  $T = 0$ . Lines are only guides for the eye.

Here is a numericalexponent; in the current study we could establish that

$$= 0.76 \quad 0.08: \quad (23)$$

This is compatible with our previous results<sup>7</sup>  $= 0.85$   $0.07$  (for the sam e model as now, for one particular value of  $E$ ) and  $= 0.85 \quad 0.02$  (for uniform slanted lattices).

Figure 9 shows the tting parameter  $L_c$  (as well as the average hop length along the electric eld,  $x_{\text{rms}}$ ) as a function of electric eld  $E$ . In the variable range hopping regime, it m ay be tted with the following law,

$$L_c = Ja \frac{E_0}{E} ; \quad J = 0.04 \quad 0.01; \quad = 0.98 \quad 0.08: \quad (24)$$

This law m ay be explained in the following way. The parameter  $L_c$  m ay be interpreted as the average percolation cluster length.<sup>7</sup> The theory of directed percolation<sup>22,23,24</sup> gives the following scaling:

$$L_c / hxi \frac{x_c}{jx_i - x_j} \quad (25)$$

W here  $hxi$  is the r m s. hop length along the eld direction ( $x_{\text{rms}}$ ),  $x_c$  is its critical value, and the critical index  $k$  should be close to  $1.73$ .<sup>24</sup> Due to the exponential nature of the hopping,  $jx_i - x_j \approx a$ , while  $x_{\text{rms}}$  should follow eld scaling similar to that given by Eq. (15). (Points in Fig. 9 show that this is true for our simulation results as well.) Thus for su ciently large  $x_{\text{rms}}$  we arrive at Eq. (24) with  $= \frac{1}{3} 1 + k = 0.911$ . This value is compatible with our numerical result, thus con iming the interpretation of  $L_c$  as the average critical cluster length.

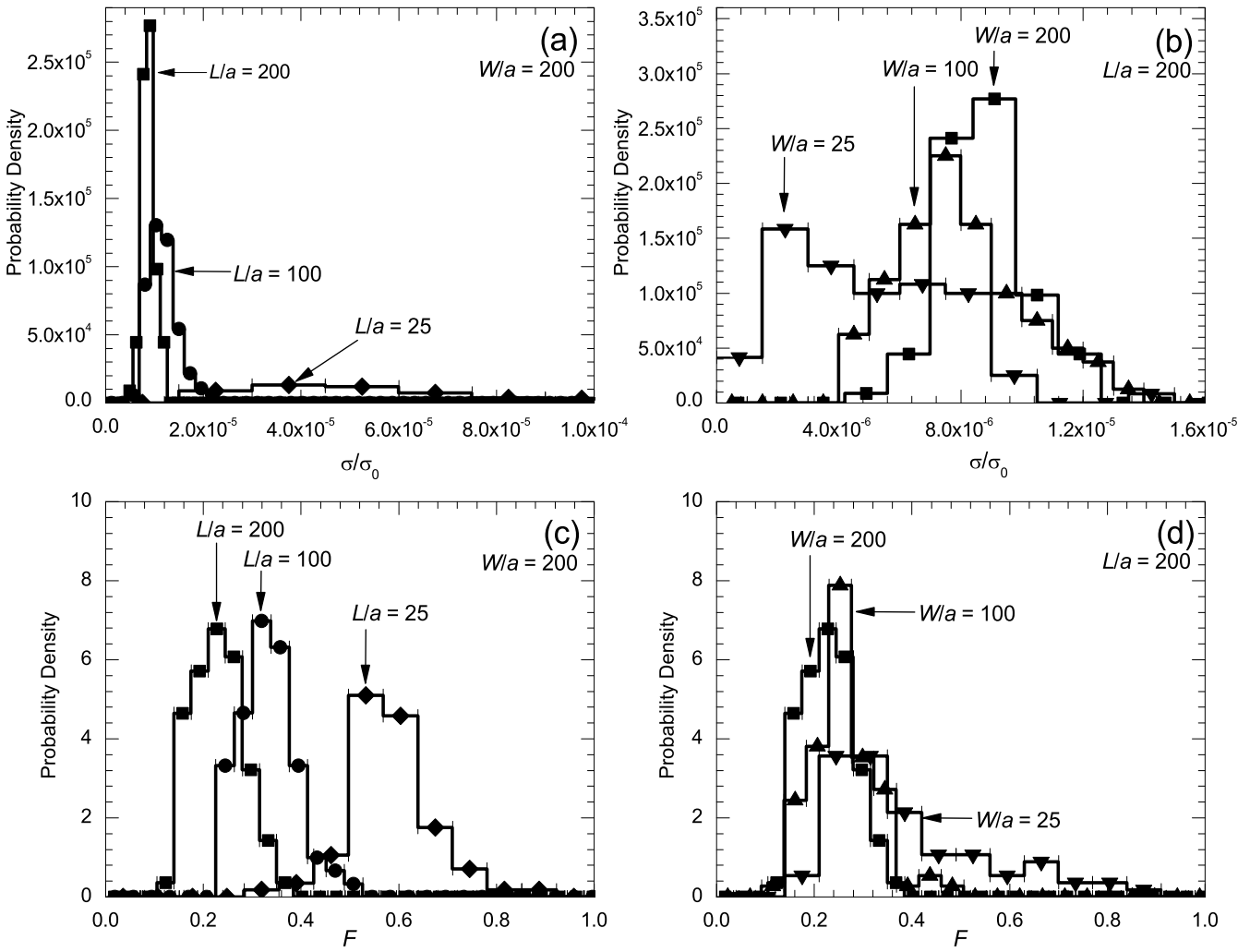


FIG. 7: Typical histograms of (a, b) dc conductivity and (c, d) Fano factor  $F$  for several samples of various length  $L$  (a, c) and width  $W$  (b, d). Parameters:  $E = E_0 = 1.09 \times 10^{-3}$ ,  $T = 0$ .

Note that in the variable range hopping regime  $L_c$  has a different field dependence, and is much larger than the average hop length. However, as the applied electric field approaches  $E_0$ , both lengths become comparable with each other and with the localization radius  $a$ .

## V. DISCUSSION

Our simulations of shot noise in 2D hopping have confirmed our earlier hypothesis<sup>7</sup> that in the absence of substantial Coulomb interaction, in broad and long samples ( $L; W \gg L_c$ ) the Fano factor  $F$  scales approximately proportionally to  $1=L$  — see Eq. (22). Other confirmations of this hypothesis have come from recent experiments with lateral transport in SiGe quantum wells<sup>25</sup> and GaAs MESFET channels.<sup>26</sup>

From the point of view of possible applications in single-electron devices,<sup>27</sup> the fact that  $F$  may be suppressed to values much less than unity, may seem en-

couraging, since it enables the use of circuit components with quasi-continuous charge transport for the compensation of random background charge. However, in order to achieve the really quasi-continuous transfer (say,  $F < 0.1$ ), the sample length  $L$  has to be an order of magnitude longer than the percolation cluster length scale  $L_c$ . On the other hand,  $L_c$  itself, especially in the most interesting case of low applied field, is much longer than the localization length  $a$  (Fig. 9) which is of the order of 1 nm in most prospective materials. Hence, it may be hard to implement sub-electron transport in components substantially smaller than 100 nm, the size probably too large for future room-temperature single-electron circuits, because of large associated stray capacitance.<sup>27</sup>

## Acknowledgments

Fruitful discussions with B. Shklovskii and D. Tsigankov are gratefully acknowledged. The work was sup-

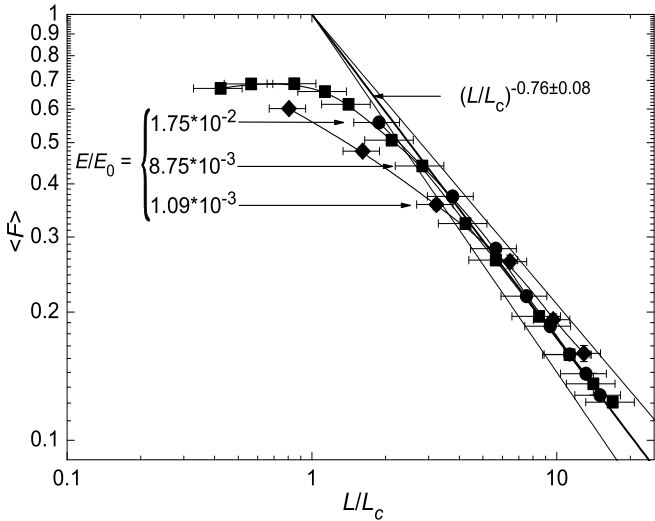


FIG. 8: Average Fano factor  $hF_i$  as a function of sample length  $L$  normalized on the average cluster size  $L_c$  (see Fig. 9 below), for several values of applied eld.  $T = 0, W = L_c$ .

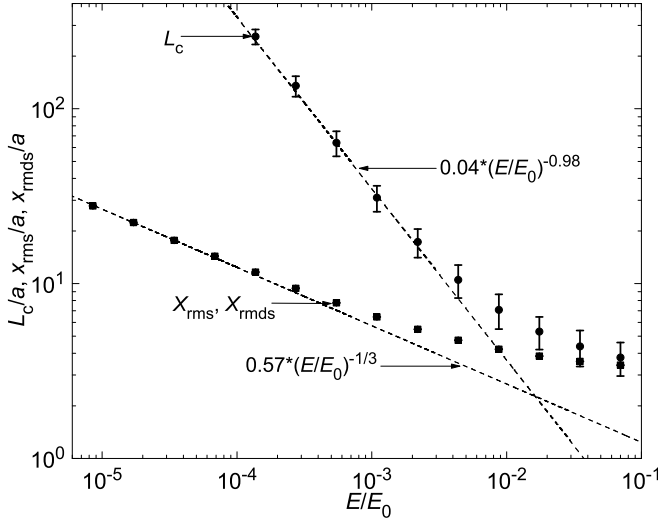


FIG. 9: The value of  $L_c$  giving the best tting of shot noise results by Eq. (22) as a function of applied electric eld (solid circles). solid squares show the sample and direction-weighed average hop length along the applied eld direction, de ned similarly to Eqs. (13) and (14).

ported in part by the Engineering Physics Program of the Office of Basic Energy Sciences at the U.S. Department of Energy. We also acknowledge the use of the following supercomputer resources: SBUs cluster Njal (purchase and installation funded by U.S. DoD's DURINT program), Oak Ridge National Laboratory's IBM SP computer Eagle (funded by the Department of Energy's Office of Science and Energy Efficiency program), and also IBM SP system Tempest at Maui High Performance Computing Center and IBM SP system Haba at NAVO Shared Resource Center (computer time granted by DoD's High Performance Computing Modernization program).

<sup>1</sup> N. F. Mott and J. H. Davies, Electronic Properties of Non-Crystalline Materials, 2nd Ed., (Oxford Univ. Press, Oxford, 1979); N. F. Mott, Conduction in Non-Crystalline Materials, 2nd Ed. (Clarendon Press, Oxford, 1993).

<sup>2</sup> B. I. Shklovskii and A. L. Efros, Electronic Properties of Doped Semiconductors (Springer, Berlin, 1984).

<sup>3</sup> Hopping Transport in Solids, edited by A. L. Efros and M. Pollak (Elsevier, Amsterdam, 1991).

<sup>4</sup> Y. A. Balantekin and M. Buttiker, Phys. Reports. 336, 2 (2000).

<sup>5</sup> K. A. Matsuoka and K. K. Likharev, Phys. Rev. B 57,

15613 (1998).

<sup>6</sup> A. N. Korotkov and K. K. Likharev, Phys. Rev. B 61, 15975 (2000).

<sup>7</sup> V. A. Sverdlov, A. N. Korotkov, and K. K. Likharev, Phys. Rev. B 63, 081302(R) (2001).

<sup>8</sup> B. I. Shklovskii, Fiz. Tekh. Poluprovodn. 6, 2335 (1972) [Sov. Phys. Semicond. 6, 1964 (1973)].

<sup>9</sup> Notice that in contrast with some prior works, we do not include the factor 2 in the exponent. This difference should be kept in mind at the level of result comparison.

<sup>10</sup> N .S .Bakhvalov, G .S .Kazacha, K .K .Likharev, and S .I .Serdyukova, Sov .Phys .JETP 68, 581 (1989).

<sup>11</sup> C .W .Asshuber, Computational Single-Electronics (Springer, Berlin, 2001), Ch .3.

<sup>12</sup> Y .A .Kinkhabwala, V .A .Sverdlov and A .N .Korotkov, (Paper in Preparation).

<sup>13</sup> W .Brenig, G .H .Dohler, and H .Heyszenau, Phil .Mag .27, 1093 (1973).

<sup>14</sup> D .N .Tsigankov and A .L .Efros, Phys .Rev .Lett .88, 176602 (2002).

<sup>15</sup> For a discussion of this issue, see Sec .4.2 of Ref .2.

<sup>16</sup> S .M .Arianer and B .I .Shklovskii, Phys .Rev .B 46, 13100 (1992).

<sup>17</sup> This result emphasizes again that the validity of the master equation approach is very limited, and for most transport characteristics this equation fails to give quantitatively correct results for any region in the [E ;T ] space.

<sup>18</sup> B .I .Shklovskii, Solid State Commun .33, 273 (1980); Sh .M .Kogan and B .I .Shklovskii, Sov .Phys .Semicond .15, 605 (1981).

<sup>19</sup> V .I .Kozub, Solid State Commun .97, 843 (1996).

<sup>20</sup> V .Ya .Pokrovskii, A .K .Savchenko, W .R .Tribe, and E .H .Linfield, Phys .Rev .B 64, 201318 (2001).

<sup>21</sup> B .I .Shklovskii, Phys .Rev .B 67, 045201 (2003).

<sup>22</sup> D .Staufer and A .Aharony, Introduction to Percolation Theory, Rev .2nd Ed ., (Taylor and Francis Inc, Philadelphia, 1994).

<sup>23</sup> S .P .Obukhov, Physica A 101, 145 (1980).

<sup>24</sup> J .W .Essam, K .DeBell, J .Adler, and F .M .Bhatti, Phys .Rev .B 33, 1982 (1986).

<sup>25</sup> V .V .Kuznetsov, E .E .Menendez, X .Zuo, G .Snider, and E .Crooke, Phys .Rev .Lett .85, 397 (2000).

<sup>26</sup> S .H .Roshko, S .S .Safonov, A .K .Savchenko, W .R .Tribe, and E .H .Linfield, Physica E 12, 861 (2002).

<sup>27</sup> K .Likharev, Proc .IEEE 87, 606 (1999).